Ethylene Oxidation

DOI: 10.1002/anie.201300496

Low-Temperature Oxidation of Ethylene over Platinum Nanoparticles Supported on Mesoporous Silica**

*Chuanxia Jiang, Kenji Hara, and Atsushi Fukuoka**

Ethylene is a gaseous volatile organic compound (VOC) that works as a plant hormone to inhibit or promote plant growth. Ethylene released from fruits, vegetables, and flowers can accelerate aging and spoiling of plants even in refrigerators at low temperature. Consequently, the removal of trace amounts of ethylene at low temperature (ca. 0 °C) is imperative.

Previously, biotechnological materials, such as soil bacteria, dry biobeds, and biofilters were applied for removal of ethylene.[1–4] However, high production costs and inefficiency in removing trace amounts of ethylene were drawbacks of these methods. Several photocatalysts have also been used,[5–8] but this resulted in limited application because of the more complicated working conditions required.

Many attempts have been made by Hao et al. to develop gold catalysts supported on Co_3O_4 for the removal of ethylene at low temperature. First, 2 wt % Au/Co_3O_4 catalyst prepared by a deposition–precipitation method showed only 7.4 % conversion of ethylene at 20 °C from a relatively low concentration (1050 ppm).[9] A more active catalyst, 2.5 wt % Au nanoparticles supported on mesoporous Co_3O_4, was later prepared by a nanocasting method, but the catalytic activity was still insufficient for complete removal of trace (50 ppm) ethylene at 0 °C despite the complicated preparation method.[10] Gold nanoparticles supported on Co_3O_4 rods recently prepared by a hydrothermal method solved the time-consuming problem of catalyst preparation; however, the method afforded no significant improvement in catalytic activity.[11] Therefore, further catalyst screening is still necessary to find sufficiently active catalysts to remove low concentrations of ethylene.

Herein, we report the catalytic performance of Pt nanoparticles supported on mesoporous silica MCM-41 for ethylene oxidation under low-temperature conditions. This study has revealed the influence of metals (Pt, Pd, Au, and Ag) and supports (MCM-41, SiO_2, Al_2O_3, ZrO_2, and TiO_2) on the catalytic performance. The Pt nanoparticles supported on MCM-41 exhibited the highest activity and demonstrated excellent durability in prolonged reaction time or recycle use. The conversion of 50 ppm ethylene over 1 wt % Pt/MCM-41 at 0 °C was over 99.8 %. To our knowledge, this is the highest conversion of ethylene oxidation at low temperature reported to date.

All of the catalysts were prepared by using a typical wet impregnation method. Characterization of the catalysts was conducted by various physicochemical methods. The structural parameters are summarized in Table 1 and Table S1 (in the Supporting Information). The small-angle X-ray diffraction (XRD) patterns of MCM-41 and 5 wt % Pt/MCM-41 (Figure S1a) are consistent with the literature,[12] and peaks appeared at (100), (110), and (200), a characteristic of a typical two-dimensional hexagonal structure of mesopores in MCM-41. This result indicates that the mesoporous structure remains unchanged after the incorporation of Pt nanoparticles. However, no such peaks were present in Pt/SiO_2, Pt/Al_2O_3, Pt/ZrO_2, and Pt/TiO_2, showing the absence of ordered structures. In the wide-angle region (Figure S1b), Pt/MCM-41 and Pt/SiO_2 have three characteristic XRD peaks at 40, 46, and 67°, which can be assigned to (111), (200), and (220) reflections of face-centered cubic (fcc) Pt crystals by comparison with the JCPDS card (No. 04-0802). The particle sizes of Pt for Pt/MCM-41 and Pt/SiO_2 estimated by the Scherrer equation from the (111) peaks are 2.4 and 5.8 nm, respectively. In contrast, no Pt peak was observed in XRD patterns of Pt/Al_2O_3, Pt/ZrO_2, and Pt/TiO_2, which may be due to the smaller Pt particles formed on these three supports as shown in the TEM images (Figure S2). The BET surface areas and pore sizes of the supports and Pt catalysts are also listed in Table 1 and Table S1. The surface areas and pore sizes of the

Table 1: Structural parameters of catalysts.

Sample	S_{BET} [$m^2 g^{-1}$][a]	D_x [nm][b]	D_{TEM} [nm][c]	CO/Pt[d]	D_c [nm][e]
5 % Pt/MCM-41	913	2.4	2.9 ± 0.7	0.38	3.0
5 % Pt/SiO_2	270	5.8	4.3 ± 1.2	0.25	4.6
5 % Pt/Al_2O_3	143	–	2.0 ± 1.0	0.44	2.6
5 % Pt/ZrO_2	72	–	1.2 ± 0.5	0.50	2.3
5 % Pt/TiO_2	52	–	2.8 ± 1.1	0.20	5.7
1 % Pt/MCM-41	820	1.7	2.0 ± 0.6	0.51	2.2
5 % Pd/MCM-41	889	3.7	–	–	–
5 % Ag/MCM-41	770	23	–	–	–
5 % Au/MCM-41	822	35	–	–	–

[a] BET (Brunauer-Emmett-Teller) surface area. [b] Particle size calculated from XRD by the Scherrer equation. [c] Particle size calculated from TEM images. [d] Uptake of CO on Pt at 50 °C. [e] Particle size calculated from $\rho_{calcd} = 1.13/D$, where D is the metallic dispersion (CO/Pt) based on CO uptake.[13,14]

[*] M. Sc. C. X. Jiang, Dr. K. Hara, Prof. Dr. A. Fukuoka
Catalysis Research Center, Hokkaido University
Kita 21 Nishi 10, Kita-ku, Sapporo, Hokkaido 001-0021 (Japan)
E-mail: fukuoka@cat.hokudai.ac.jp
M. Sc. C. X. Jiang
Graduate School of Chemical Sciences and Engineering,
Hokkaido University
Kita 13 Nishi 8, Kita-ku, Sapporo, Hokkaido 060-8628 (Japan)

[**] C.X.J. acknowledges MEXT of Japan for a scholarship.

Supporting information for this article is available on the WWW under http://dx.doi.org/10.1002/anie.201300496.

Pt catalysts were almost the same as the pure supports, indicating high homogeneity of the pore size and no plugging of the pores by Pt nanoparticles.

A typical TEM image of the supported Pt catalysts is shown in Figure 1 (and Figure S2) with the corresponding particle size distribution from more than two hundred particles. Ordered mesoporous channels and highly monodispersed Pt nanoparticles were observed for Pt/MCM-41 in Figure 1. The Pt particle sizes obtained from the TEM image are in the range of 1.2–4.3 nm (Table 1). Similarly, the corresponding particle sizes (D_c) based on CO chemisorption are 2.3–5.7 nm, which were calculated by the literature method.[13,14] Therefore, in these samples, we deduce most of the Pt surface is exposed to the gas phase.

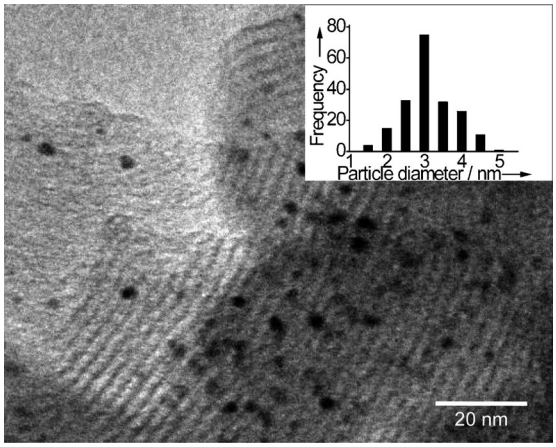

Figure 1. TEM image of 5% Pt/MCM-41. Inset: Particle size distribution.

Figure 2a shows the light-off curves of ethylene conversion over different metals on MCM-41. Complete oxidation of ethylene was observed on Pt/MCM-41 over a wide range of reaction temperatures (25–200°C). However, ethylene conversion was less than 40% for Pd/MCM-41 and Au/MCM-41 at 25–50°C. An increase in reaction temperature afforded over 99.8% conversion above 145°C for Pd/MCM-41 and 96% conversion at 200°C for Au/MCM-41. At any given temperature, the Ag/MCM-41 catalyst provided only 40% ethylene conversion. From these results, it can be concluded that Pt is the most effective metal for ethylene oxidation under these conditions.

The effect of the support was also investigated using Pt catalysts supported on MCM-41, SiO_2, Al_2O_3, ZrO_2, and TiO_2 (Figure 2b). The catalytic activities were ranked as follows: Pt/MCM-41 > Pt/SiO_2 > Pt/Al_2O_3 > Pt/TiO_2, Pt/ZrO_2. The difference in catalytic activity between Pt/MCM-41 and Pt/SiO_2 might be attributed to the difference in particle size and surface area of Pt. As shown in Table 1, the particle size of Pt for Pt/MCM-41 is smaller than that for Pt/SiO_2. Normally, higher BET surface areas of the support afford smaller Pt particles, which induce higher catalytic activities.[15] In this regard, it is interesting that extremely low ethylene oxidation efficiency was obtained with Pt catalysts supported on Al_2O_3, ZrO_2, or TiO_2, where particle sizes are smaller than active Pt/MCM-41 and Pt/SiO_2 catalysts.

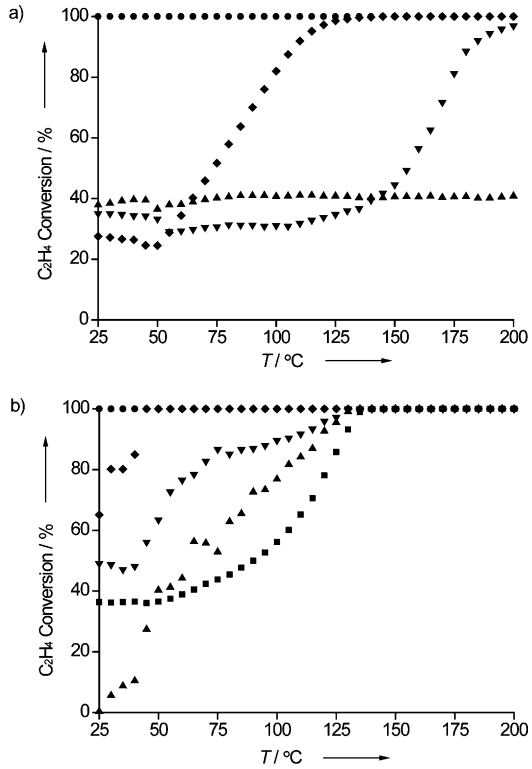

Figure 2. a) Light-off curves of catalytic ethylene conversion over different metals supported on MCM-41 (● Pt/MCM-41; ◆ Pd/MCM-41; ▼ Au/MCM-41; ▲ Ag/MCM-41) and b) Pt nanoparticles on different supports (● Pt/MCM-41; ◆ Pt/SiO_2; ▼ Pt/Al_2O_3; ▲ Pt/ZrO_2; ■ Pt/TiO). Pt loading: 5 wt%; space velocity (SV): 1500 mL h^{-1} g^{-1}; catalyst: 0.20 g; C_2H_4: 0.32 vol%; O_2: 20 vol%; N_2: 5 vol%; He balance.

In this study, 2 wt% and 1 wt% Pt/MCM-41 were also prepared for investigation under more practical conditions with trace ethylene (50 ppm) at ambient or lower temperature (25 or 0°C). As shown in Table S2, the ethylene conversion reached 97% by using 2 wt% Pt/MCM-41, which was higher than the reported data under almost the same reaction conditions for Au/Co_3O_4 catalyst.[10,11] The conversion of 50 ppm ethylene with 1 wt% Pt/MCM-41 remained approximately 100% for more than 12 h at 25°C, showing great potential applicability to warehouse storage (Figure 3a). In addition, we applied 1 wt% Pt/MCM-41 catalyst for ethylene oxidation at 0°C (Figure 3b). Notably, over 99.8% ethylene conversion was accomplished under these conditions and the conversion of ethylene was maintained for more than 1 h. The gradual deactivation observed in Figure 3b is attributed to adsorption of water on the catalyst surface, but high catalytic activity was recovered by heating the catalyst at 200°C under a He flow for 1 h. No size or structural change was observed for the spent catalyst in XRD (Figure S3) and TEM (Figure S4) analysis.

Mechanistic studies were performed for the ethylene oxidation on Pt/MCM-41 catalyst by using diffuse reflectance infrared Fourier transform (DRIFT) spectroscopy. All spectra were obtained after subtraction of the background

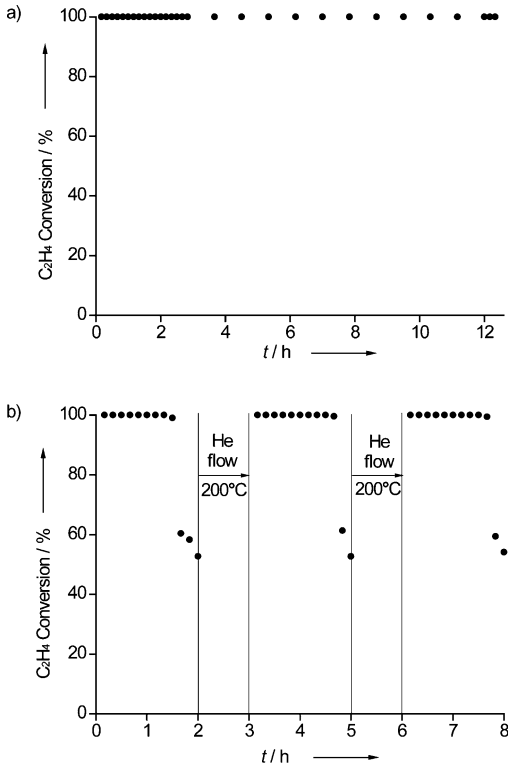

Figure 3. a) Catalytic performance and durability of Pt/MCM-41 at 25 °C and b) 0 °C. Pt loading: 1 wt%; SV: 1500 mL h^{-1} g^{-1}; catalyst: 0.40 g; C_2H_4: 50 ppm; O_2: 20 vol%; N_2: 5 vol%; He balance.

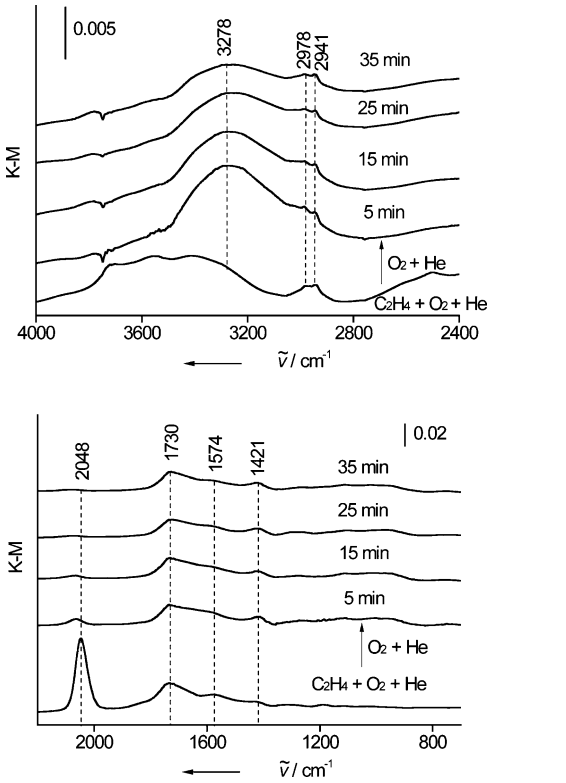

Figure 4. Two sections of the DRIFT spectra of adsorption of C_2H_4 on 5% Pt/MCM-41 catalyst. The sample was pretreated in H_2 at 200 °C for 1 h. After cooling to 50 °C, it was exposed to a flow of C_2H_4 (0.2 mL min^{-1}) + O_2 (4 mL min^{-1}) + He (16 mL min^{-1}) for 30 min, then the flow of C_2H_4 was stopped while maintaining O_2 + He flow for 35 min. Spectra vertically off-set for clarity.

spectrum under He atmosphere. The bottom lines in Figure 4 display IR spectra of Pt/MCM-41 catalyst under a flow of C_2H_4 (0.2 mL min^{-1}) + O_2 (4 mL min^{-1}) + He (16 mL min^{-1}) at 50 °C. No C_2H_4 band was found in these spectra, which demonstrates the fast conversion of C_2H_4 to other species. The strong band near 2048 cm^{-1} is assignable to linear CO species on the Pt surface,[12,16] which is slightly shifted to lower frequency than that obtained under a flow of pure CO (2085 cm^{-1}, Figure S5) probably as a result of lower CO coverage.[17,18] The band at 3278 cm^{-1} resulted from the formation of H_2O. Moreover, bands at 2978, 1730, and 1421 cm^{-1} can be assigned to physical adsorption of formic acid on the MCM-41 surface,[19] while two other bands at 2941 and 1574 cm^{-1} are attributed to adsorption of formate species on MCM-41 (Figure S6c).[19,20] When the C_2H_4 flow was stopped and the O_2 + He flow was continued, the intensity of the band corresponding to linear CO on Pt rapidly decreased whereas the formic acid and the formate species on MCM-41 still remained even after 35 min. It is notable that a control DRIFT measurement by flowing vapor of HCHO as a probe molecule into Pt/MCM-41 catalyst (Figure S6b) gave similar peaks to those observed in Figure 4. Therefore, these results imply that HCHO initially adsorbed on Pt is decomposed to CO, but part of HCHO is oxidized into HCOOH to be spilled over onto MCM-41 as a form of formic acid and formate species. All band assignments are listed in Table S3.

Based on the DRIFT experiment, a reaction mechanism is tentatively proposed for the C_2H_4 oxidation on Pt/MCM-41. As depicted in Scheme S1, C_2H_4 and O_2 react quickly to form HCHO. HCHO adsorbed on Pt is then decomposed mainly into CO and H species, which react with O species to give CO_2 and H_2O, respectively. In this process, a small amount of formic acid is generated from HCHO on Pt as a by-product and spilled over onto MCM-41.

Another finding in the present study is the support effect on catalytic activity as already noted in Figure 2b. The same DRIFT experiments using the less-effective catalysts (Pt/Al_2O_3, Pt/ZrO_2, and Pt/TiO_2; Figure S7) revealed the reason for the effect. It was found that the disappearance of the CO band observed on Al_2O_3-, ZrO_2-, and TiO_2-supported Pt catalysts is much slower than that for Pt/MCM-41 and Pt/SiO_2 under the same conditions. Accordingly, the facile oxidation of CO over Pt on silica supports is the key to the high catalytic activity in the complete oxidation of C_2H_4. Such fast CO oxidation might be promoted by the presence of surface silanol in a related mechanism proposed for the preferential oxidation of CO in excess H_2 (PROX).[12,16] Similar high activity of supported Au catalysts for CO oxidation has been reported.[21]

In conclusion, we have found that Pt nanoparticles supported on mesoporous silica MCM-41 serve as an excellent catalyst for complete oxidation of ethylene at low temperature with high activity and durability. As a typical demonstration under practical conditions, the conversion of ethylene over 1 wt% Pt/MCM-41 at 0 °C was over 99.8%,

which is higher than any previous results. IR experiments suggest that the main pathway for C_2H_4 oxidation on Pt/MCM-41 is fast oxidation of C_2H_4 to HCHO and subsequent decomposition of HCHO into CO and H, and their oxidation to CO_2 and H_2O. The effective catalytic performance of silica supports could be attributed to facile oxidation of CO absorbed on Pt prepared on these supports. The detailed mechanism of support effects and kinetic studies are now under investigation.

Experimental Section

All the catalysts were prepared by using the impregnation method. $H_2PtCl_6{\cdot}6H_2O$, $PdCl_2$, $HAuCl_4{\cdot}4H_2O$, and $AgNO_3$ were used as metal precursors. MCM-41, SiO_2 (Fuji Silysia, Cariact Q-10), γ-Al_2O_3 (Nishio Kogyo, A-11), TiO_2 (JRC-TIO-4), and mesoporous ZrO_2 were used as catalyst supports. Typically, the support material (1.0 g) was impregnated with an aqueous solution (50 mL) containing the required amount of metal precursor salts. The mixture was stirred for 18 h, evaporated and dried under vacuum overnight. The resulting solid was calcined under O_2 flow at 200 °C for 2 h, and then reduced under H_2 flow at 200 °C for 2 h.

The catalytic oxidation of C_2H_4 was performed in a stainless steel tubular fixed-bed reactor (i.d. = 4 mm) under atmospheric pressure. Each catalyst (0.20 g, 40–60 mesh) loaded in the reactor was pretreated under a H_2 stream (30 mL min^{-1}) at 200 °C for 1 h before use. The reactant gas mixture [C_2H_4 (99.99 %) 0.32 vol %, O_2 (99.999 %) 20 vol %, N_2 (99.999 %) 5 vol %, He (99.999 %) balance] was fed to the reactor using mass flow controllers to achieve the desired flow rates. After reaching a steady state, typically in ca. 1 h, the reaction temperature was gradually increased from room temperature to 200 °C (1 °C min^{-1}), and the outlet gas was analyzed at every 5 °C interval using an online gas chromatograph [Agilent 3000A Micro GC equipped with thermal conductivity detector (TCD) and a column of molecular sieves 5 A (10 m) and Plot U (8 m)]. The catalytic performance of 1 wt % Pt/MCM-41 (0.40 g, 40–60 mesh) was also investigated at 0 °C with 50 ppm of C_2H_4. The detection limit of C_2H_4 was 0.1 ppm in the present analysis.

DRIFT measurements were conducted at 50 °C on a PerkinElmer Spectrum 100 (resolution 2–4 cm^{-1}, integration 64 times) equipped with an MCT detector and a S.T. Japan DRIFT heating chamber. In each experiment, sample powder (6.0 mg) was placed in a DRIFT cell with a KBr window. The experimental details can be seen in Supporting Information.

Received: January 20, 2013
Revised: March 28, 2013
Published online: May 3, 2013

Keywords: ethylene · heterogeneous catalysis · oxidation · platinum · silica

[1] J. A. M. De-Bont, *Anton. Leeuw. Int. J. G.* **1976**, *42*, 59 – 71.
[2] L. Elsgaard, *Appl. Environ. Microbiol.* **1998**, *64*, 4168 – 4173.
[3] B. De Heyder, A. Overmeire, H. V. Langenhove, W. Verstraete, *Biotechnol. Bioeng.* **1994**, *44*, 642 – 648.
[4] L. Elsgaard, *Appl. Environ. Microbiol.* **2000**, *66*, 3878 – 3882.
[5] D. R. Park, J. L. Zhang, K. Ikeue, H. Yamashita, M. Anpo, *J. Catal.* **1999**, *185*, 114 – 119.
[6] D. R. Park, B. J. Ahn, H. S. Park, H. Yamashita, M. Anpo, *Korean J. Chem. Eng.* **2001**, *18*, 930 – 934.
[7] S. Kim, Y. Watabe, T. Aida, H. Niiyama, *J. Chem. Eng. Jpn.* **2005**, *38*, 828 – 834.
[8] H. G. Ahn, B. M. Choi, D. J. Lee, *J. Nanosci. Nanotechnol.* **2006**, *6*, 3599 – 3603.
[9] J. J. Li, C. Y. Ma, X. Y. Xu, J. J. Yu, Z. P. Hao, S. Z. Qiao, *Environ. Sci. Technol.* **2008**, *42*, 8947 – 8951.
[10] C. Y. Ma, Z. Mu, J. J. Li, Y. G. Jin, J. Cheng, G. Q. Lu, Z. P. Hao, S. Z. Qiao, *J. Am. Chem. Soc.* **2010**, *132*, 2608 – 2613.
[11] W. J. Xue, Y. F. Wang, P. Li, Z. T. Liu, Z. P. Hao, C. Y. Ma, *Catal. Commun.* **2011**, *12*, 1265 – 1268.
[12] S. J. Huang, K. Hara, A. Fukuoka, *Chem. Eur. J.* **2012**, *18*, 4738 – 4747.
[13] J. R. Anderson, *Structure of Metallic Catalysts*, Academic Press, New York, **1975**, pp. 358 – 363.
[14] G. Bergeret, P. Gallezot in *Handbook of Heterogeneous Catalysis*, *Vol. 2* (Eds.: G. Ertl, H. Knözinger, J. Weitkamp), VCH, Weinheim, **1997**, pp. 439 – 464.
[15] M. C. Kung, R. J. Davis, H. H. Kung, *J. Phys. Chem. C* **2007**, *111*, 11767 – 11775.
[16] A. Fukuoka, J. Kimura, T. Oshio, Y. Sakamoto, M. Ichikawa, *J. Am. Chem. Soc.* **2007**, *129*, 10120 – 10125.
[17] J. F. E. Gootzen, A. H. Wonders, W. Visscher, J. A. R. Vanveen, *Langmuir* **1997**, *13*, 1659 – 1667.
[18] K. Tanaka, M. Shou, H. He, X. Y. Shi, X. L. Zhang, *J. Phys. Chem. C* **2009**, *113*, 12427 – 12433.
[19] G. X. Li, M. J. Ridd, F. P. Larkins, *Aust. J. Chem.* **1991**, *44*, 623 – 626.
[20] G. J. Millar, C. H. Rochester, K. C. Waugh, *J. Catal.* **1995**, *155*, 52 – 58.
[21] M. Haruta, T. Kobayashi, H. Sano, N. Yamada, *Chem. Lett.* **1987**, *16*, 405 – 408.

